



HAL
open science

A fictitious domain decomposition method for a nonlinear bonded structure

Amina Chorfi, Jonas Koko, Olivier Bodart

► **To cite this version:**

Amina Chorfi, Jonas Koko, Olivier Bodart. A fictitious domain decomposition method for a nonlinear bonded structure. *Mathematics and Computers in Simulation*, 2021, 189, pp.114-125. 10.1016/j.matcom.2020.09.003 . hal-04136725

HAL Id: hal-04136725

<https://hal.science/hal-04136725>

Submitted on 22 Jul 2024

HAL is a multi-disciplinary open access archive for the deposit and dissemination of scientific research documents, whether they are published or not. The documents may come from teaching and research institutions in France or abroad, or from public or private research centers.

L'archive ouverte pluridisciplinaire **HAL**, est destinée au dépôt et à la diffusion de documents scientifiques de niveau recherche, publiés ou non, émanant des établissements d'enseignement et de recherche français ou étrangers, des laboratoires publics ou privés.



Distributed under a Creative Commons Attribution - NonCommercial - NoDerivatives 4.0 International License

A fictitious domain decomposition method for a nonlinear bonded structure

Amina CHORFI¹, Jonas KOKO¹, and Olivier BODART²

¹LIMOS, Université Clermont-Auvergne – CNRS UMR 6158, BP 10448, 63000
Clermont-Ferrand, France

²ICJ, Université Saint-Etienne – CNRS UMR 5208, CS 82301, 42023 Saint-Etienne, France

July 25, 2020

Abstract

We study a fictitious domain decomposition method for a nonlinearly bonded structure. Starting with a strongly convex unconstrained minimization problem, we introduce an interface unknown such that the displacement problems on each subdomain become uncoupled in the saddle-point equations. The interface unknown is eliminated and a Uzawa conjugate gradient domain decomposition method is derived from the saddle-point equations of the stabilized Lagrangian functional. To avoid interface fitted meshes we use a fictitious domain approach, inspired by XFEM, which consists in cutting the finite element basis functions around the interface. Some numerical experiments are proposed to illustrate the efficiency of the proposed method.

Keywords: Domain decomposition; bonded structure; saddle-point problem; elasticity.

1 Introduction

A bonded structure consists of two elastic adherents bonded by a thin adhesive layer. In real world applications, bonded structures can be encountered in aircraft industrie (composite structure, e.g., metal/polymer); civil engineering (concrete block/mortar); geology (granite/clay or quartzite/magma). To avoid numerical difficulties due the geometrical and mechanical differences between the adhesive and the adherents, simplified models obtained by asymptotic analysis are used. In such models, the adhesive layer disappears, replaced by a transmission condition. We refer to [5, 24] and references therein for asymptotic analysis of bonded structures. With simplified models, the domain decomposition approach applies in a natural way since the subdomains and the interface are already defined [18, 11].

In this paper we study a bonded structure composed of linear elastic adherents and a nonlinear adhesive layer. Our model generalizes the linear model studied in [12, 11] and the nonlinear model studied in [5, 6]. Starting with a strongly convex unconstrained minimization problem, we introduce an interface unknown such that the displacement

problems on each subdomain become uncoupled if the multiplier is known. Then we eliminate the auxiliary unknown to obtain a reduced Lagrangian functional. We derive a Uzawa conjugate gradient algorithm based on the saddle-point equations of the stabilized Lagrangian functional. For our domain decomposition method, we use a fictitious domain approach to avoid the generation of compatible meshes. The fictitious domain method we use was initiated by [16] for the Poisson equation (see also [4, 7, 15]) and allows the use of different degrees of freedom for the interface multiplier and the subdomains. The approach is inspired by XFEM [22] since it consists partially in cutting the finite element basis function around the interface. But unlike XFEM, the finite element function spaces are not enriched with singular functions, even though [1] shows a equivalence between both methods.

The paper is organized as follows. In Section 2, we described the model problem. In Section 3, we derive the dual problem and a Uzawa-type domain decomposition algorithm in a continuous level. In Section 4 we introduce a standard finite element discretization and a Uzawa conjugate gradient algorithm. In Section 5 we present the stabilized fictitious domain discretization and the corresponding Uzawa conjugate gradient algorithm. Finally in Section 6, we carry out some numerical experiments to illustrate the behavior of the proposed method.

2 Model problem

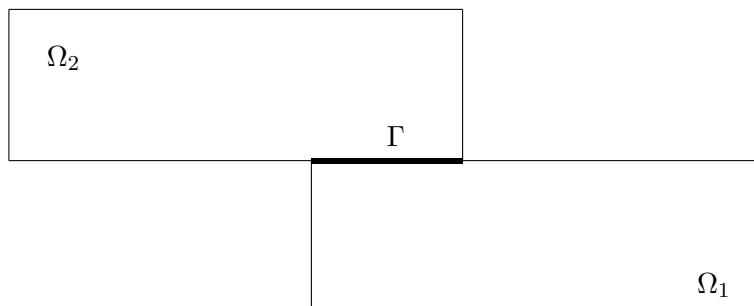


Figure 1: A bonded structure : Ω_1 and Ω_2 sub-domains (adherents), Γ interface (thin adhesive layer)

We consider, in \mathbb{R}^2 , a system of two isotropic (linear) elastic bodies Ω_1 and Ω_2 , bonded along their common boundary Γ by a thin adhesive layer, see Figure 1. The common boundary Γ is assumed to be nonempty surface of positive measure. Let \mathbf{u}_i be the displacement field of the body Ω_i . We set $\mathbf{u} = (\mathbf{u}_1, \mathbf{u}_2)$ the displacement field of the bonded

structure and $[\mathbf{u}] = (\mathbf{u}_1 - \mathbf{u}_2)|_\Gamma$ the displacement jump across Γ . Under small deformations assumption, constitutive equations are, for each body Ω_i ,

$$\begin{aligned}\sigma_i(\mathbf{u}_i) &= 2\mu_i\varepsilon_i(\mathbf{u}_i) + \lambda_i(\operatorname{div}(\mathbf{u}_i))\mathbb{I}_{\mathbb{R}^2}, \\ \varepsilon_i(\mathbf{u}_i) &= \frac{1}{2}(\nabla\mathbf{u}_i + \nabla\mathbf{u}_i^\top),\end{aligned}$$

where μ_i and λ_i are the Lamé constants for Ω_i . We assume that each body Ω_i is subjected to applied body forces \mathbf{f}_i and, for simplicity, Dirichlet boundary conditions are taken on a part of its boundary Γ_i , with $\operatorname{meas}(\Gamma_i) > 0$. With the above assumptions, the local equilibrium equations, for the bonded structure, are

$$-\operatorname{div}\sigma_i(\mathbf{u}_i) = \mathbf{f}_i, \quad \text{in } \Omega_i, \quad i = 1, 2 \quad (2.1)$$

$$\mathbf{u}_i = 0, \quad \text{on } \Gamma_i, \quad i = 1, 2, \quad (2.2)$$

$$\sigma_i(\mathbf{u}_i)\mathbf{n}_i = (-1)^i |K[\mathbf{u}]|^{p-2} K^2[\mathbf{u}], \quad i = 1, 2 \text{ on } \Gamma. \quad (2.3)$$

Eq. (2.3) is the transmission conditions, modelling the thin adhesive layer, in which \mathbf{n}_i is the unit outward normal to Ω_i , $p \in [2, +\infty[$, $|\cdot|$ is the Euclidean norm, and K is the bonding tensor assumed to be constant, bounded, *symmetric* and strictly positive. The transmission condition (2.3) generalized the transmission conditions studied in [5, 11, 18, 17, 6, 24]. Indeed, if $p = 2$ we find the linear transmission condition studied in [11, 18, 17], i.e.

$$\sigma_i(\mathbf{u}_i)\mathbf{n}_i = (-1)^i \tilde{K}[\mathbf{u}], \quad i = 1, 2,$$

with $\tilde{K} = K^2$. If $K = \kappa\mathbb{I}_{\mathbb{R}^2}$ we recover the model studied in [5, 6, 24], i.e.

$$\sigma_i(\mathbf{u}_i)\mathbf{n}_i = (-1)^i \tilde{\kappa} |\mathbf{u}|^{p-2} [\mathbf{u}], \quad i = 1, 2,$$

with $\tilde{\kappa} = \kappa^p$.

Let us define, for $i = 1, 2$, the subspaces

$$\mathbf{V}_i = \{\mathbf{v}_i \in (H^1(\Omega_i))^2; \mathbf{v}_i = 0 \text{ on } \Gamma_i\}$$

and the forms

$$\begin{aligned}a_i(\mathbf{u}_i, \mathbf{v}_i) &= \int_{\Omega_i} \sigma_i(\mathbf{u}_i) : \varepsilon(\mathbf{v}_i) \, dx; \quad \mathbf{u}_i, \mathbf{v}_i \in \mathbf{V}_i \\ \mathbf{f}_i(\mathbf{v}_i) &= \int_{\Omega_i} \mathbf{f}_i \cdot \mathbf{v}_i \, dx; \quad \mathbf{v}_i \in \mathbf{V}_i,\end{aligned} \quad (2.4)$$

assuming that $\mathbf{f}_i \in (L^2(\Omega_i))^2$. We set $\mathbf{V} = \mathbf{V}_1 \times \mathbf{V}_2$ and

$$\mathbf{a}(\mathbf{u}, \mathbf{v}) = \sum_{i=1}^2 a_i(\mathbf{u}_i, \mathbf{v}_i),$$

$$\mathbf{f}(\mathbf{v}) = \sum_{i=1}^2 \mathbf{f}_i(\mathbf{v}_i).$$

The scalar product over Γ is denoted by $(\cdot, \cdot)_{\Gamma}$. The variational formulation of the problem (2.1)-(2.3) is therefore:

Find $\mathbf{u} = (\mathbf{u}_1, \mathbf{u}_2) \in \mathbf{V}_1 \times \mathbf{V}_2$ such that

$$\mathbf{a}(\mathbf{u}, \mathbf{v}) + (|K[\mathbf{u}]|^{p-2}K[\mathbf{u}], K[\mathbf{v}])_{\Gamma} = \mathbf{f}(\mathbf{v}), \quad \forall \mathbf{v} \in \mathbf{V}. \quad (2.5)$$

using the symmetry property of K .

For the derivation of the domain decomposition method, we need a minimization formulation of (2.5). To this end, we introduce the total potential energy of the adherents

$$J(\mathbf{v}) = \frac{1}{2} \mathbf{a}(\mathbf{v}, \mathbf{v}) - \mathbf{f}(\mathbf{v}). \quad (2.6)$$

The thin adhesive layer is characterized by the following non quadratic potential energy

$$J_{\Gamma}(\mathbf{v}) = \frac{1}{p} \int_{\Gamma} |K[\mathbf{v}]|^p d\Gamma. \quad (2.7)$$

The bonded structure problem (2.5) can be formulated as the following minimization problem.

Find $\mathbf{u} \in \mathbf{V}$ such that

$$J(\mathbf{u}) + J_{\Gamma}(\mathbf{u}) \leq J(\mathbf{v}) + J_{\Gamma}(\mathbf{v}), \quad \forall \mathbf{v} \in \mathbf{V} \quad (2.8)$$

The functional $J + J_{\Gamma}$ being strictly convex, coercive and Gâteaux-differentiable, we have the following classical theorem (see e.g., [10, 21]).

Theorem 2.1. *The minimization problem (2.8) has a unique solution \mathbf{u} verifying (2.5).*

3 Dualization and Lagrangian formulation

To simplify the nonlinear structure of (2.8) by decoupling the elasticity subproblems, we have to introduce an auxiliary interface unknown linked to \mathbf{u} through a linear constraint. To handle this constraint, we use a Lagrange multiplier and reduce (2.8) to a saddle-point problem.

3.1 Constrained optimization formulation

To transform the unconstrained minimization problem (2.8) into a constrained minimization problem we introduce the (interface) auxiliary unknown $\phi = K[\mathbf{u}]$. We then obtain

Find $(\mathbf{u}, \phi) \in \mathbf{V} \times \mathbf{L}^p(\Gamma)$ such that

$$J(\mathbf{u}) + J_{\Gamma}(\phi) \leq J(\mathbf{v}) + J_{\Gamma}(\varphi), \quad \forall (\mathbf{v}, \varphi) \in \mathbf{V} \times \mathbf{L}^p(\Gamma), \quad (3.1)$$

$$K[\mathbf{u}] - \phi = 0, \quad (3.2)$$

where the interface functional is now

$$J_\Gamma(\phi) = \frac{1}{p} \int_\Gamma |\phi|^p d\Gamma.$$

With (3.1)-(3.2), we associate the Lagrangian functional

$$\mathcal{L}(\mathbf{u}, \phi; \boldsymbol{\lambda}) = J(\mathbf{v}) + J_\Gamma(\phi) + (K[\mathbf{u}] - \phi, \boldsymbol{\lambda})_\Gamma \quad (3.3)$$

such that the solution to (3.1)-(3.2) reduces to the following saddle-point problem

Find $(\mathbf{u}, \phi; \boldsymbol{\lambda}) \in \mathbf{V} \times \mathbf{L}^p(\Gamma) \times \mathbf{L}^q(\Gamma)$ such that

$$\mathcal{L}(\mathbf{u}, \phi; \boldsymbol{\mu}) \leq \mathcal{L}(\mathbf{u}, \phi; \boldsymbol{\lambda}) \leq \mathcal{L}(\mathbf{v}, \varphi; \boldsymbol{\lambda}), \quad \forall (\mathbf{v}, \varphi; \boldsymbol{\mu}) \in \mathbf{V} \times \mathbf{L}^p(\Gamma) \times \mathbf{L}^q(\Gamma), \quad (3.4)$$

where q is such that $1/p + 1/q = 1$.

Theorem 3.1. *The saddle-point problem (3.4) has a unique solution $(\mathbf{u}, \phi; \boldsymbol{\lambda})$ in $\mathbf{V} \times \mathbf{L}^p(\Gamma) \times \mathbf{L}^q(\Gamma)$ with (\mathbf{u}, ϕ) solution of (3.1)-(3.2) and $\boldsymbol{\lambda} = |K[\mathbf{u}]|^{p-2} K[\mathbf{u}]$.*

Proof. Since $J + J_\Gamma$ is strictly convex and the constraints are linear, the saddle point exists and is unique (see, e.g., [9, §.III.3] or [23, §28]). The saddle-point $(\mathbf{u}, \phi, \boldsymbol{\lambda})$ of \mathcal{L} is solution of the following Euler-Lagrange equations

$$\sum_i a_i(\mathbf{u}_i, \mathbf{v}_i) = \sum_i \mathbf{f}_i(\mathbf{v}_i) - (\boldsymbol{\lambda}, K[\mathbf{v}])_\Gamma, \quad \forall \mathbf{v} \in \mathbf{V}, \quad (3.5)$$

$$(|\phi|^{p-2} \phi, \varphi)_\Gamma = (\boldsymbol{\lambda}, \varphi)_\Gamma, \quad \forall \varphi \in \mathbf{L}^q(\Gamma) \quad (3.6)$$

$$(\boldsymbol{\mu}, K[\mathbf{u}] - \phi)_\Gamma = 0, \quad \forall \boldsymbol{\mu} \in \mathbf{L}^q(\Gamma). \quad (3.7)$$

From(3.7) we get $\phi = K[\mathbf{u}]$. Substituting this result in (3.6) we obtain the optimal value of $\boldsymbol{\lambda}$. \square

The main advantage of the Lagrangian formulation is that, if $\boldsymbol{\lambda}$ is known then (3.5) is uncoupled and

$$(\boldsymbol{\lambda}, K[\mathbf{v}])_\Gamma = (K\boldsymbol{\lambda}, [\mathbf{v}])_\Gamma,$$

K being symmetric. Then (3.5) can be set in each subdomain independently, that is

$$a_i(\mathbf{u}_i, \mathbf{v}_i) = \mathbf{f}_i(\mathbf{v}_i) + (-1)^i (K\boldsymbol{\lambda}, \mathbf{v}_i)_\Gamma, \quad \forall \mathbf{v}_i \in \mathbf{V}_i, \quad i = 1, 2.$$

As in [6], we can set $\varphi \leftarrow \boldsymbol{\lambda}$ and $\varphi \leftarrow \phi$ in (3.6) to get

$$|\phi|^{p-2} \phi \cdot \boldsymbol{\lambda} = |\boldsymbol{\lambda}|^2, \quad (3.8)$$

$$|\phi|^p = \boldsymbol{\lambda} \cdot \phi. \quad (3.9)$$

Using (3.9) in Eq. (3.8) we obtain

$$|\phi| = |\boldsymbol{\lambda}|^{1/(p-1)}$$

and

$$\phi = \lambda/|\lambda|^{(p-2)/p-1}. \quad (3.10)$$

The terms involving ϕ in \mathcal{L} become ($q = p/(p-1)$)

$$\begin{aligned} \frac{1}{p} \int_{\Gamma} |\phi|^p d\Gamma &= \frac{1}{p} \int_{\Gamma} |\lambda|^q d\Gamma, \\ \int_{\Gamma} \lambda \cdot \phi d\Gamma &= \int_{\Gamma} |\lambda|^q d\Gamma, \end{aligned}$$

such that the Lagrangian functional (3.3) becomes

$$\mathcal{L}(\mathbf{u}, \boldsymbol{\lambda}) = J(\mathbf{u}) + (\boldsymbol{\lambda}, K[\mathbf{u}])_{\Gamma} - \frac{1}{q} \int_{\Gamma} |\boldsymbol{\lambda}|^q d\Gamma. \quad (3.11)$$

The saddle-point of the reduced Lagrangian (3.11) is the solution of the reduced Euler-Lagrange equations

$$a_i(\mathbf{u}_i, \mathbf{v}_i) = \mathbf{f}_i(\mathbf{v}_i) + (-1)^i (K\boldsymbol{\lambda}, \mathbf{v}_i)_{\Gamma}, \quad \forall \mathbf{v}_i \in \mathbf{V}_i, \quad (3.12)$$

$$(|\boldsymbol{\lambda}|^{q-2} \boldsymbol{\lambda}, \boldsymbol{\mu})_{\Gamma} = (K[\mathbf{u}], \boldsymbol{\mu})_{\Gamma}, \quad \forall \boldsymbol{\mu} \in \mathbf{L}^q(\Gamma). \quad (3.13)$$

Our domain decomposition method is based on the reduced Lagrangian functional (3.11) through its saddle-point equations (3.12)-(3.13).

3.2 Dual problem

The dual problem of (3.1)-(3.2) is obtained by eliminating the primal unknown \mathbf{u} . To this end we assume that $\mathbf{u} = \mathbf{u}(\boldsymbol{\lambda})$ is solution of the uncoupled sub-problems

$$a_i(\mathbf{u}_i, \mathbf{v}_i) = \mathbf{f}_i(\mathbf{v}_i) + (-1)^i (K\boldsymbol{\lambda}, \mathbf{v}_i)_{\Gamma}, \quad \forall \mathbf{v}_i \in \mathbf{V}_i, \quad i = 1, 2; \quad (3.14)$$

that is,

$$\sum_i a_i(\mathbf{u}_i, \mathbf{v}_i) = \sum_i \mathbf{f}_i(\mathbf{v}_i) - (\boldsymbol{\lambda}, K[\mathbf{v}])_{\Gamma}, \quad \forall \mathbf{v}_i \in \mathbf{V}_i. \quad (3.15)$$

Setting $\mathbf{v}_i \leftarrow \mathbf{u}_i$ in (3.15) and substituting the result in (3.11) we get the dual functional

$$J^*(\boldsymbol{\lambda}) = -\frac{1}{q} \int_{\Gamma} |\boldsymbol{\lambda}|^q d\Gamma - \frac{1}{2} \sum_i a_i(\mathbf{u}_i(\boldsymbol{\lambda}), \mathbf{u}_i(\boldsymbol{\lambda})). \quad (3.16)$$

The dual problem is therefore

Find $\boldsymbol{\lambda} \in \mathbf{L}^q(\Gamma)$ such that

$$J^*(\boldsymbol{\lambda}) \geq J^*(\boldsymbol{\mu}), \quad \forall \boldsymbol{\mu} \in \mathbf{L}^q(\Gamma). \quad (3.17)$$

Note that the bilinear forms a_i are coercive, i.e., there exists $m_i > 0$ such that

$$m_i \|\mathbf{u}_i\|_{H^1(\Omega_i)} \leq a_i(\mathbf{u}_i, \mathbf{u}_i), \quad \forall \mathbf{u}_i \in \mathbf{V}_i.$$

It follows that, from (3.14) and the compact embedding of $H^1(\Omega)$ into $L^q(\Gamma)$,

$$\| \mathbf{u} \|_{H^1(\Omega)} \leq c \| \boldsymbol{\lambda} \|_{L^q(\Gamma)}, \quad \forall \boldsymbol{\lambda} \in \mathbf{L}^q(\Gamma), \quad (3.18)$$

where c is a positive constant. On the other hand, a_i is continuous, i.e., there exists $n_i > 0$ such that

$$a_i(\mathbf{u}_i, \mathbf{u}_i) \leq n_i \| \mathbf{u}_i \|_{H^1(\Omega_i)}, \quad \forall \mathbf{u}_i \in \mathbf{V}_i. \quad (3.19)$$

We deduce from (3.18)-(3.19) that $J^*(\boldsymbol{\lambda}) \rightarrow -\infty$ as $\| \boldsymbol{\lambda} \|_{L^q(\Gamma)} \rightarrow +\infty$. Then J^* is strictly concave and coercive for $p \geq 2$. It follows that (3.17) as unique solution (see, e.g., [10, 21]).

3.3 Domain decomposition algorithm

We easily deduce, from (3.15), that the mapping $\boldsymbol{\lambda} \mapsto \mathbf{u}(\boldsymbol{\lambda})$ is linear and $\mathbf{u}(\boldsymbol{\lambda} + \rho \boldsymbol{\mu}) = \mathbf{u} + \rho \mathbf{w}$ with \mathbf{w} the solution of the sensitivity problem

$$a_i(\mathbf{w}_i, \mathbf{v}_i) = (-1)^i (K \boldsymbol{\mu}, \mathbf{v}_i)_\Gamma, \quad \forall \mathbf{v}_i \in \mathbf{V}_i, \quad i = 1, 2. \quad (3.20)$$

Then the first directional derivative of J^* is given by

$$\frac{\partial}{\partial \boldsymbol{\lambda}} J^*(\boldsymbol{\lambda}) \cdot \boldsymbol{\mu} = -(|\boldsymbol{\lambda}|^{q-2} \boldsymbol{\lambda}, \boldsymbol{\mu})_\Gamma - \sum_i a_i(\mathbf{u}_i, \mathbf{w}_i).$$

Setting $\mathbf{v}_i \leftarrow \mathbf{u}_i$ in (3.20) we obtain

$$\frac{\partial}{\partial \boldsymbol{\lambda}} J^*(\boldsymbol{\lambda}) \cdot \boldsymbol{\mu} = -(|\boldsymbol{\lambda}|^{q-2} \boldsymbol{\lambda}, \boldsymbol{\mu})_\Gamma + (K[\mathbf{u}], \boldsymbol{\mu})_\Gamma.$$

Hence the gradient of the dual functional

$$\boldsymbol{\gamma} := \nabla J^*(\boldsymbol{\lambda}) = K[\mathbf{u}] - |\boldsymbol{\lambda}|^{q-2} \boldsymbol{\lambda}, \quad \forall \boldsymbol{\lambda} \in \mathbf{L}^q(\Gamma). \quad (3.21)$$

With the gradient available, we can design a maximization algorithm for J^* of the form

$$\boldsymbol{\lambda}^{k+1} = \boldsymbol{\lambda}^k + \rho_k \boldsymbol{\mu}^k,$$

where $\boldsymbol{\mu}^k$ is a search direction, that is, verifying

$$\frac{\partial}{\partial \boldsymbol{\lambda}} J^*(\boldsymbol{\lambda}) \cdot \boldsymbol{\mu} > 0.$$

If $p = 2$, then $\mathbf{L}^q(\Gamma) = \mathbf{L}^2(\Gamma)$ is a Hilbert space. A search direction can be computed from (3.21). If $p > 2$, then $\mathbf{L}^q(\Gamma)$ is no more a Hilbert space but a search direction can be constructed using a Riesz mapping from $\mathbf{L}^q(\Gamma)$ to $\mathbf{L}^p(\Gamma)$ (see, e.g., [6, 8]).

After computing the search direction, we have to determine the step size ρ^* by solving (for ρ)

$$0 = \frac{\partial}{\partial \boldsymbol{\lambda}} J^*(\boldsymbol{\lambda} + \rho \boldsymbol{\mu}) \cdot \boldsymbol{\mu} = (K[\mathbf{u}] + \rho K[\mathbf{w}] - |\boldsymbol{\lambda} + \rho \boldsymbol{\mu}|^{q-2} (\boldsymbol{\lambda} + \rho \boldsymbol{\mu}), \boldsymbol{\mu})_\Gamma. \quad (3.22)$$

For $p = q = 2$, a straightforward calculation yields to

$$\rho^* = -\frac{(K[\mathbf{u}] - \boldsymbol{\lambda}, \boldsymbol{\mu})_\Gamma}{(K[\mathbf{w}] - \boldsymbol{\mu}, \boldsymbol{\mu})_\Gamma}.$$

If $p > 2$, (3.22) is strongly nonlinear and a numerical method for nonlinear equations must be used.

A continuous domain decomposition algorithm that generates a maximizing sequence for J^* is described in Algorithm 1. A detailed and discrete version will be given in the next section.

Algorithm 1 Uzawa-type domain decomposition method.

Assuming that $\boldsymbol{\lambda}^k$ is known

- Compute the search direction $\boldsymbol{\mu}^k$
- Solve, for $\mathbf{w}^k = (\mathbf{w}_1, \mathbf{w}_2) \in \mathbf{V}_1 \times \mathbf{V}_2$, the uncoupled sensitivity subproblems

$$a_i(\mathbf{w}_i^k, \mathbf{v}_i) = (-1)^i (K\boldsymbol{\mu}^k, \mathbf{v}_i)_\Gamma, \quad \forall \mathbf{v}_i \in \mathbf{V}_i, \quad i = 1, 2.$$

- Compute the step size ρ_k by solving (3.22)
 - Update the unknowns: $\boldsymbol{\lambda}^{k+1} = \boldsymbol{\lambda}^k + \rho_k \boldsymbol{\mu}^k$ and $\mathbf{u}_i^{k+1} = \mathbf{u}_i^k + \rho_k \mathbf{w}_i^k$, for $i = 1, 2$.
-

4 Finite element approximation

We assume that Ω_i has a polygonal Lipschitz-continuous boundary, so it can be entirely triangulated. We also assume that $\Gamma = \partial\Omega_1 \cap \partial\Omega_2$ is a straight line. Let $\mathcal{T}_h = \mathcal{T}_{1h} \cup \mathcal{T}_{2h}$ be a triangulation of $\Omega = \Omega_1 \cup \Omega_2$, consisting of triangles T not crossing the bonding interface Γ . We also assume that the meshes match on Γ , i.e., the nodes opposite to one another have the same coordinates so that the solution jump $[\mathbf{u}]$ can be computed easily. We define finite element spaces of displacements

$$\mathbf{V}_{ih} = \{ \mathbf{v} \in \mathcal{C}^0(\overline{\Omega}_i)^2; \mathbf{v}|_T \in P_1(T)^2, \forall T \in \mathcal{T}_{ih}; v = 0 \text{ on } \Gamma_i \} \subset \mathbf{V}_i, \quad i = 1, 2,$$

where $P_1(T)$ is the space of polynomials of degree ≤ 1 on T . The triangulation \mathcal{T}_h induces on Γ a decomposition \mathcal{I}_h into intervals I . We then define the finite element space for the interface unknowns

$$\boldsymbol{\Lambda}_h = \{ \boldsymbol{\lambda}_h \in \mathcal{C}^0(\Gamma)^2; \boldsymbol{\lambda}_h|_I \in P_1(I)^2, \forall I \in \mathcal{I}_h \} \subset \mathbf{L}^q(\Gamma).$$

The space $\boldsymbol{\Lambda}_h$ will be the space of the interface Lagrange multipliers. Since $\boldsymbol{\Lambda}_h \subset \mathbf{L}^2(\Gamma)$, we can work in $\mathbf{L}^2(\Gamma)$ as in [12]. In [6], it is shown that the convergence obtained in $\mathbf{L}^2(\Gamma)$ with $\boldsymbol{\Lambda}_h$ is also valid for $\mathbf{L}^q(\Gamma)$.

For $\boldsymbol{\lambda}_h \in \boldsymbol{\Lambda}_h$, the discrete dual functional is then

$$J^*(\boldsymbol{\lambda}_h) = -\frac{1}{q} \int_{\Gamma} |\boldsymbol{\lambda}_h|^q d\Gamma - \frac{1}{2} \sum_i a_i(\mathbf{u}_{ih}(\boldsymbol{\lambda}_h), \mathbf{u}_{ih}(\boldsymbol{\lambda}_h)), \quad (4.1)$$

where $\mathbf{u}_{ih}(\boldsymbol{\lambda}_h) \in \mathbf{V}_{ih}$ is the solution of the discrete (uncoupled) displacement subproblems

$$a_i(\mathbf{u}_{ih}, \mathbf{v}_{ih}) = \mathbf{f}_i(\mathbf{v}_{ih}) + (-1)^i (K\boldsymbol{\lambda}_h, \mathbf{v}_{ih})_{\Gamma}, \quad \forall \mathbf{v}_{ih} \in \mathbf{V}_{ih}. \quad (4.2)$$

For a search direction $\boldsymbol{\mu}_h \in \boldsymbol{\Lambda}_h$, the discrete uncoupled sensitivity subproblems are

$$a_i(\mathbf{w}_{ih}, \mathbf{v}_{ih}) = (-1)^i (K\boldsymbol{\mu}_h, \mathbf{v}_{ih})_{\Gamma}, \quad \forall \mathbf{v}_{ih} \in \mathbf{V}_{ih}, \quad i = 1, 2.$$

In the discrete setting, a search direction is computed from (3.21). Since J^* is a general nonlinear functional, one of the best search direction is a conjugate gradient direction. For the Fletcher-Reeves version, the conjugate gradient is constructed as follows, at iteration k .

$$\beta_k = \|\boldsymbol{\gamma}_h^{k+1}\|_{L^2(\Gamma)}^2 / \|\boldsymbol{\gamma}_h^k\|_{L^2(\Gamma)}^2, \quad (4.3)$$

$$\boldsymbol{\mu}_h^{k+1} = \boldsymbol{\gamma}_h^{k+1} + \beta_k \boldsymbol{\mu}_h^k. \quad (4.4)$$

After computing the search direction, we have to determine the step size ρ_k by solving (for ρ) a discrete version of (3.22), i.e.

$$(K[\mathbf{u}_h] + \rho K[\mathbf{w}_h] - |\boldsymbol{\lambda}_h + \rho \boldsymbol{\mu}_h|^{q-2} (\boldsymbol{\lambda}_h + \rho \boldsymbol{\mu}_h), \boldsymbol{\mu}_h)_{\Gamma} = 0.$$

As in [6], we use the following fixed-point procedure

$$\rho^{n+1} = \frac{(K[\mathbf{u}_h] - |\boldsymbol{\lambda}_h + \rho^n \boldsymbol{\mu}_h|^{q-2} \boldsymbol{\lambda}_h, \boldsymbol{\mu}_h)_{\Gamma}}{(K[\mathbf{w}_h] - |\boldsymbol{\lambda}_h + \rho^n \boldsymbol{\mu}_h|^{q-2} \boldsymbol{\mu}_h, \boldsymbol{\mu}_h)_{\Gamma}}, \quad n \geq 0. \quad (4.5)$$

With the results above, the Uzawa conjugate gradient domain decomposition for a bonded structure is described in Algorithm 2.

5 Fictitious domain approach

To avoid the generation of meshes which coincide on the interface, we chose the fictitious domain approach in which the choice of the degrees of freedom for the multiplier on Γ is made independently of the mesh. The fictitious domain used here has been first introduced by Haslinger and Renard [16] for the Poisson problem.

5.1 Interface mesh

We set $\Omega = \Omega_1 \cup \Omega_2$ and let \mathcal{T} be a triangulation of Ω using piecewise linear finite elements which are independent of the location of the interface Γ . In practice, the triangulation \mathcal{T}_h is generated without taking into account the interface Γ . Let T be a triangle intersected by

Algorithm 2 Uzawa conjugate gradient domain decomposition method.

Step 0. $\boldsymbol{\lambda}_h^0$ is given, compute $\mathbf{u}_h^0 = (\mathbf{u}_{1h}^0, \mathbf{u}_{2h}^0) \in \mathbf{V}_{1h} \times \mathbf{V}_{2h}$ such that

$$a_i(\mathbf{u}_{ih}^0, \mathbf{v}_{ih}) = \mathbf{f}_i(\mathbf{v}_{ih}) + (-1)^i (K \boldsymbol{\lambda}_h^0, \mathbf{v}_{ih})_\Gamma, \quad \forall \mathbf{v}_{ih} \in \mathbf{V}_{ih}, \quad i = 1, 2.$$

$$\boldsymbol{\gamma}_h^0 = K[\mathbf{u}_h^0] - |\boldsymbol{\lambda}_h^0|^{q-2} \boldsymbol{\lambda}_h^0$$

$$\boldsymbol{\mu}_h^0 = \boldsymbol{\gamma}_h^0$$

Step $k \geq 0$. Assuming that $\boldsymbol{\lambda}_h^k$ is known

- Solve, for $\mathbf{w}_h^k = (\mathbf{w}_{1h}, \mathbf{w}_{2h})$, the uncoupled sensitivity subproblems

$$a_i(\mathbf{w}_{ih}^k, \mathbf{v}_{ih}) = (-1)^i (K \boldsymbol{\mu}_h^k, \mathbf{v}_{ih})_\Gamma, \quad \forall \mathbf{v}_{ih} \in \mathbf{V}_{ih}, \quad i = 1, 2.$$

- Compute the step size ρ_k using (4.5)
- Update the unknowns

$$\begin{aligned} \boldsymbol{\lambda}_h^{k+1} &= \boldsymbol{\lambda}_h^k + \rho_k \boldsymbol{\mu}_h^k \\ \mathbf{u}_{ih}^{k+1} &= \mathbf{u}_{ih}^k + \rho_k \mathbf{w}_{ih}^k, \quad i = 1, 2. \end{aligned}$$

- Gradient : $\boldsymbol{\gamma}_h^{k+1} = K[\mathbf{u}_h^{k+1}] - |\boldsymbol{\lambda}_h^{k+1}|^{q-2} \boldsymbol{\lambda}_h^{k+1}$
 - Conjugate gradient direction: $\boldsymbol{\mu}_h^{k+1} = \boldsymbol{\gamma}_h^{k+1} + \beta_k \boldsymbol{\mu}_h^k$
- $$\beta_k = \|\boldsymbol{\gamma}_h^{k+1}\|^2 \|\boldsymbol{\gamma}_h^k\|^{-2}$$
-

the interface and thus consists of two sub-elements $T_1 = \Omega_1 \cap K$ and $T_2 = \Omega_2 \cap K$. Assume that $T = \{a, b, c\}$, with $a, b \in \Omega_1$ and $c \in \Omega_2$. Following [7, 15], T is split into two copies $T_1 = \{a_1, b_1, c_1\}$ and $T_2 = \{a_2, b_2, c_2\}$, using fictitious nodes $c_1 \in \Omega_1$ and $a_2, b_2 \in \Omega_2$. We then obtain two independent meshes, one completely covering Ω_1 and the other completely covering Ω_2 .

For the displacement field approximation, the triangles that are not crossed by Γ are handled in the standard way. For a triangle T_i crossed by Γ the displacement field is approximated by $\mathbf{u}_h(\mathbf{x}) = \sum \phi_j(\mathbf{x}) H_i(\mathbf{x}) \mathbf{u}_j$, where ϕ_j are the standard piecewise linear basis functions, \mathbf{u}_j are nodal values and H_i is the Heaviside function

$$H_i(\mathbf{x}) = \begin{cases} 1 & \text{if } \mathbf{x} \in \Omega_i \\ 0 & \text{if } \mathbf{x} \notin \Omega_i. \end{cases}$$

Let us consider some discrete spaces $\tilde{\mathbf{V}}_h \subset (H^1(\Omega))^2$ and $\tilde{\Lambda}_h \subset (L^2(\Omega))^2$ defined by

$$\tilde{\mathbf{V}}_h = \{ \mathbf{v}_h \in \mathcal{C}^0(\bar{\Omega})^2 \mid \mathbf{v}_h|_{\Gamma_0} = 0, \mathbf{v}_h|_T \in P_1(T), \forall T \in \mathcal{T}_h \},$$

$$\tilde{\Lambda}_h = \left\{ \boldsymbol{\mu}_h \in \mathcal{C}^0(\bar{\Omega})^2 \mid \boldsymbol{\mu}_h|_T \in P_1(T), \forall T \in \mathcal{T}_h \right\},$$

where $\Gamma_0 = \Gamma_1 \cup \Gamma_2$, and $P_1(T)$ is the space of polynomials of degree ≤ 1 on T . We then define \mathbf{V}_{ih} and Λ_h as the restriction of $\tilde{\mathbf{V}}_h$ and $\tilde{\Lambda}_h$ to Ω_i and Γ , i.e.

$$\mathbf{V}_{ih} := \tilde{\mathbf{V}}_h|_{\Omega_i}, \quad \Lambda_h := \tilde{\Lambda}_h|_{\Gamma}.$$

Unlike the fictitious method with distributed Lagrange multipliers (see, e.g., [13, 14]), the Lagrange multiplier nodes are the intersection of Γ with the edges of the triangles crossed.

5.2 Stabilization

The assumption $\mathbf{u}_h(\boldsymbol{\lambda}_h)$ is the solution of

$$a_i(\mathbf{u}_{ih}, \mathbf{v}_{ih}) = \mathbf{f}_i(\mathbf{v}_{ih}) - (K\boldsymbol{\lambda}_h, [\mathbf{v}_h])_{\Gamma}, \quad \forall \mathbf{v}_{ih} \in \mathbf{V}_{ih},$$

used for the derivation of the domain decomposition Algorithm 2 implies that

$$-K\boldsymbol{\lambda}_h = \sigma_1(\mathbf{u}_{1h}) \cdot \mathbf{n}_1 = -\sigma_2(\mathbf{u}_{2h}) \cdot \mathbf{n}_2$$

that is

$$\boldsymbol{\lambda}_h = -K^{-1}\sigma_1(\mathbf{u}_{1h}) \cdot \mathbf{n}_1 = K^{-1}\sigma_2(\mathbf{u}_{2h}) \cdot \mathbf{n}_2. \quad (5.1)$$

To ensure the convergence of the Lagrange multiplier for any interface configuration, Barbosa-Hughes [2, 3] propose to add, to the Lagrangian functional, an additional "penalty" term which takes into account (5.1). We then consider the following Lagrangian functional, for $\alpha > 0$,

$$\mathcal{L}_\alpha(\mathbf{u}_h, \boldsymbol{\lambda}_h) = \mathcal{L}(\mathbf{u}_h, \boldsymbol{\lambda}_h) - \frac{\alpha}{2} \int_{\Gamma} |\boldsymbol{\lambda}_h + K^{-1}\sigma_1(\mathbf{u}_{1h})\mathbf{n}_1|^2 d\Gamma - \frac{\alpha}{2} \int_{\Gamma} |\boldsymbol{\lambda}_h - K^{-1}\sigma_2(\mathbf{u}_{2h})\mathbf{n}_2|^2 d\Gamma, \quad (5.2)$$

where \mathcal{L} is the reduced Lagrangian functional (3.11). Since the additional terms in (5.2) are quadratic, the dual functional, the gradient and the optimal step size can be computed easily, following the same procedure as in Section 3.

Computing the first derivatives of (5.2), we obtain the saddle point equations

Find $(\mathbf{u}_h, \boldsymbol{\lambda}_h) \in \mathbf{V}_h \times \Lambda_h$ such that

$$\mathbf{a}_\alpha(\mathbf{u}_h, \mathbf{v}_h) + b_\alpha(\mathbf{v}_h, \boldsymbol{\lambda}_h) = \mathbf{f}(\mathbf{v}_h), \quad \forall \mathbf{v}_h \in \mathbf{V}_h, \quad (5.3)$$

$$\mathbf{b}_\alpha(\mathbf{u}_h, \boldsymbol{\mu}) - c(\boldsymbol{\lambda}_h, \boldsymbol{\mu}_h) = 0, \quad \forall \boldsymbol{\mu}_h \in \Lambda_h, \quad (5.4)$$

where

$$\mathbf{a}_\alpha(\mathbf{u}_h, \mathbf{v}_h) = \sum_i a(\mathbf{u}_{ih}, \mathbf{v}_{ih}) - \alpha \sum_i (K^{-1}\sigma_i(\mathbf{u}_{ih})\mathbf{n}_i, K^{-1}\sigma_i(\mathbf{v}_{ih})\mathbf{n}_i)_{\Gamma} \quad (5.5)$$

$$\begin{aligned} \mathbf{b}_\alpha(\boldsymbol{\lambda}_h, \mathbf{v}_h) &= (\boldsymbol{\lambda}, K[\mathbf{v}_h])_\Gamma - \alpha \sum_i (-1)^i (K^{-1} \sigma_i(\mathbf{v}_{ih}) \mathbf{n}_i, \boldsymbol{\lambda}_h)_\Gamma \\ c(\boldsymbol{\lambda}_h, \boldsymbol{\mu}_h) &= 2\alpha(\boldsymbol{\lambda}_h, \boldsymbol{\mu}_h)_\Gamma \end{aligned}$$

The negative quadratic term in (5.5) deteriorates the coerciveness of the bilinear form a_α if α is too large. Assuming that $\mathbf{u}_h(\boldsymbol{\lambda}_h)$ is the solution of (5.3), we obtain the stabilized sensitivity problem

$$\mathbf{a}_\alpha(\mathbf{u}_h, \mathbf{v}_h) = -(\boldsymbol{\mu}_h, K[\mathbf{v}_h] + \alpha \sum_i (-1)^i K^{-1} \sigma_i(\mathbf{v}_{ih}) \mathbf{n}_i)_\Gamma, \quad \forall \mathbf{v}_h \in \mathbf{V}_h, \quad (5.6)$$

and the stabilized dual functional

$$J_\alpha^*(\boldsymbol{\lambda}_h) = -\frac{1}{2} a_\alpha(\mathbf{u}_h, \mathbf{u}_h) - \frac{1}{q} \int_\Gamma |\boldsymbol{\lambda}_h|^q d\Gamma - \alpha \int_\Gamma |\boldsymbol{\lambda}_h|^2 d\Gamma.$$

The fixed-point scheme (4.5) for the optimal stepsize becomes

$$\rho^0 = -\frac{(K[\mathbf{u}_h] - 2\alpha \boldsymbol{\lambda}_h, \boldsymbol{\mu}_h)_\Gamma}{(K[\mathbf{w}_h] - 2\alpha \boldsymbol{\mu}, \boldsymbol{\mu})_\Gamma}, \quad (5.7)$$

$$\rho^{n+1} = -\frac{(K[\mathbf{u}_h] - (2\alpha + |\boldsymbol{\lambda}_h + \rho^n \boldsymbol{\mu}_h|^{q-2}) \boldsymbol{\lambda}_h, \boldsymbol{\mu}_h)_\Gamma}{(K[\mathbf{w}_h] - (2\alpha + |\boldsymbol{\lambda}_h + \rho^n \boldsymbol{\mu}_h|^{q-2}) \boldsymbol{\mu}_h, \boldsymbol{\mu}_h)_\Gamma}, \quad n \geq 0 \quad (5.8)$$

The initial step size ρ^0 corresponds to the quadratic case (i.e. $p = 2$).

5.3 Stabilized domain decomposition algorithm

To simplify the presentation of the algorithm, we set

$$\begin{aligned} a_{\alpha i}(\mathbf{u}_{ih}, \mathbf{v}_{ih}) &= a_i(\mathbf{u}_{ih}, \mathbf{v}_{ih}) - \alpha (K^{-1} \sigma_i(\mathbf{u}_{ih}) \mathbf{n}_i, K^{-1} \sigma_i(\mathbf{v}_{ih}) \mathbf{n}_i)_\Gamma \\ b_{\alpha i}(\boldsymbol{\lambda}_h, \mathbf{v}_{ih}) &= (K \boldsymbol{\lambda}_h, \mathbf{v}_{ih} + \alpha K^{-1} \sigma_i(\mathbf{v}_{ih}) \mathbf{n}_i)_\Gamma, \end{aligned}$$

so that the subdomain problems can be written

$$a_{\alpha i}(\mathbf{u}_{ih}, \mathbf{v}_{ih}) = \mathbf{f}(\mathbf{v}_{ih}) + (-1)^i b_{\alpha i}(\boldsymbol{\lambda}_h, \mathbf{v}_{ih}), \quad \forall \mathbf{v}_{ih} \in \mathbf{V}_{ih}, \quad i = 1, 2.$$

The stabilized Uzawa conjugate gradient domain decomposition method for a nonlinearly bonded structure is described in Algorithm 3.

6 Numerical experiments

We now study the numerical behavior of Algorithm 3. We have implemented Algorithm 3 in MATLAB, using vectorized assembling functions and the mesh generator provided in [19, 20], on a computer running Linux (Ubuntu 16.04) with 3.00GHz clock frequency and 32GB RAM. The test problem used is designed in order to illustrate the numerical behavior of the algorithms more than to model actual bonded structures.

Algorithm 3 Stabilized Uzawa conjugate gradient domain decomposition method.

Step 0. $\alpha > 0$ and $\boldsymbol{\lambda}_h^0$ is given, compute $\mathbf{u}_h^0 = (\mathbf{u}_{1h}^0, \mathbf{u}_{2h}^0) \in \mathbf{V}_{1h} \times \mathbf{V}_{2h}$ such that

$$a_{\alpha i}(\mathbf{u}_{ih}^0, \mathbf{v}_{ih}) = \mathbf{f}(\mathbf{v}_{ih}) + (-1)^i b_{\alpha i}(\boldsymbol{\lambda}_h^0, \mathbf{v}_{ih}), \quad \forall \mathbf{v}_{ih} \in \mathbf{V}_{ih}, \quad i = 1, 2.$$

Compute $\boldsymbol{\gamma}_h^0 \in \boldsymbol{\Lambda}_h$ such that

$$(\boldsymbol{\gamma}_h^0, \tilde{\boldsymbol{\gamma}}_h)_\Gamma = (K[\mathbf{u}_h^0] - (2\alpha + |\boldsymbol{\lambda}_h^0|^{q-2})\boldsymbol{\lambda}_h^0, \tilde{\boldsymbol{\gamma}})_\Gamma, \quad \forall \tilde{\boldsymbol{\gamma}}_h \in \boldsymbol{\Lambda}_h.$$

Initial search direction: $\boldsymbol{\mu}_h^0 = \boldsymbol{\gamma}_h^0$

Step $k \geq 0$. Assuming that $\boldsymbol{\lambda}_h^k, \mathbf{u}_h^k, \boldsymbol{\mu}_h^k$ are known

- Solve, for \mathbf{w}_h^k , the uncoupled sensitivity subproblems

$$a_{\alpha i}(\mathbf{w}_{ih}, \mathbf{v}_{ih}) = (-1)^i b_{\alpha i}(\boldsymbol{\mu}_h^k, \mathbf{v}_{ih}), \quad \forall \mathbf{v}_{ih} \in \mathbf{V}_{ih}, \quad i = 1, 2.$$

- Compute the step size ρ_k using (5.7)-(5.8)
- Update the unknowns

$$\begin{aligned} \boldsymbol{\lambda}_h^{k+1} &= \boldsymbol{\lambda}_h^k + \rho_k \boldsymbol{\mu}_h^k \\ \mathbf{u}_{ih}^{k+1} &= \mathbf{u}_{ih}^k + \rho_k \mathbf{w}_{ih}^k, \quad i = 1, 2. \end{aligned}$$

- New gradient: $\boldsymbol{\gamma}_h^{k+1} = K[\mathbf{u}_h^{k+1}] - (2\alpha + |\boldsymbol{\lambda}_h^{k+1}|^{q-2})\boldsymbol{\lambda}_h^{k+1}$.
 - New direction: $\boldsymbol{\mu}_h^{k+1} = \boldsymbol{\gamma}_h^{k+1} + \beta_k \mathbf{w}_h^k$ with $\beta_k = \|\boldsymbol{\gamma}_h^{k+1}\|^2 \|\boldsymbol{\gamma}_h^k\|^{-2}$.
-

The test problem used is illustrated in figure 2, derived from [18]. The adherents and the interface are

$$\Omega_1 = (-10, 0) \times (0, 50), \quad \Omega_2 = (0, 10) \times (0, 50), \quad \Gamma = \{0\} \times (0, 50).$$

The materials are isotropic and the materials constants of the adherents are

$$E_1 = 50000\text{MPA}, \quad \nu_1 = 0.3, \quad E_2 = 25000\text{MPA} \quad \nu_2 = 0.3.$$

There are no volume forces, i.e. $\mathbf{f}_i = 0$ for $i = 1, 2$. On Γ_i , Dirichlet boundary conditions $\mathbf{u}_i = 0$ are prescribed while Γ_i^σ is subjected to surface traction

$$\sigma_i(\mathbf{u}_i)\mathbf{n}_i = -100 \begin{pmatrix} 0 \\ 1 \end{pmatrix} \text{ on } \Gamma_i^\sigma, \quad i = 1, 2,$$

with \mathbf{n}_i the unit outward normal. The bonding tensor K , modelling the thin adhesive layer, is given by

$$K = \frac{(E^*)^{1/p}}{2(1 + \nu^*)} \begin{bmatrix} \frac{(1-\nu^*)}{1-2\nu^*} & 0 \\ 0 & 1 \end{bmatrix}$$

where $E^* = 1800\text{MPa}$ and $\nu^* = 0.35$. Note that $K^p \rightarrow 0$ when $p \rightarrow +\infty$.

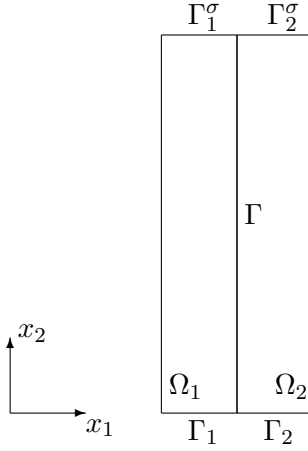


Figure 2: Geometry of the bonded structure problem

6.1 Implementation details

We use the following stopping criterion for Algorithm 3

$$\| \boldsymbol{\gamma}_h^k \|_{L^2(\Gamma)} < 10^{-5} \| \boldsymbol{\gamma}_h^0 \|_{L^2(\Gamma)} .$$

For the step size, we stop the fixed-point scheme if the relative error on ρ^n becomes smaller than 10^{-10} . Without a suitable $\boldsymbol{\lambda}_h^0$, the number of iterations required by Algorithm 3 could become prohibitive, for $p > 2$. We use the following procedure for the initialization step of the algorithm. We first solve

$$a_{\alpha i}(\tilde{\mathbf{u}}_{ih}, \mathbf{v}_{ih}) = \mathbf{f}(\mathbf{v}_{ih}), \quad \forall \mathbf{v}_{ih} \in \mathbf{V}_{ih}, \quad i = 1, 2.$$

Then we compute the initial value of the Lagrange multiplier using Theorem 3.1, i.e.

$$\boldsymbol{\lambda}_h^0 = |K[\tilde{\mathbf{u}}_h]|^{p-2} K[\tilde{\mathbf{u}}_h]$$

We use the following formula (derived from [7]) for the stabilization parameter

$$\alpha = 10^{-10} h \frac{1 - 2\tilde{\nu}}{\tilde{E}}$$

where h is the mesh size, $\tilde{\nu} = \max(\nu_1, \nu_2)$ and $\tilde{E} = \max(E_1, E_2)$.

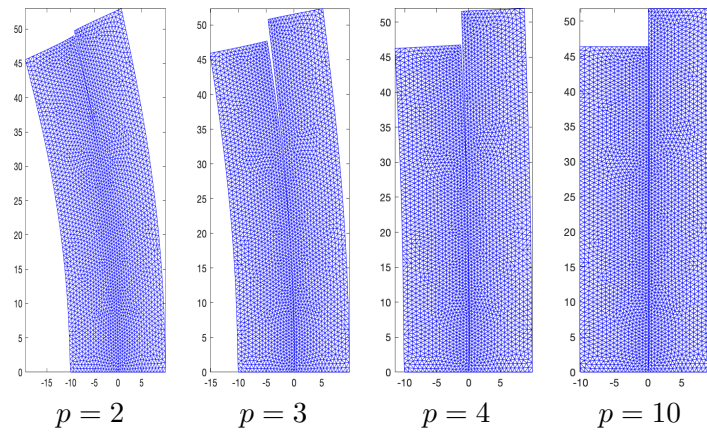


Figure 3: Deformed configurations for various values of p , obtained using standard FEM

6.2 Standard FEM Versus Fictitious domain decomposition

We first consider a discretization with a uniform mesh composed of 20×51 nodes and 101 interface nodes. We also consider a standard FEM discretization with 2×1658 nodes and 105 interface nodes. In Figure 3-4 we plot the deformed configurations obtained with both approaches. One can notice that both methods produce the same results and the bonding effect disappears for large values of p . Figure 5, representing the interface normal stress, confirms that the bonding effect disappears for large values of p .

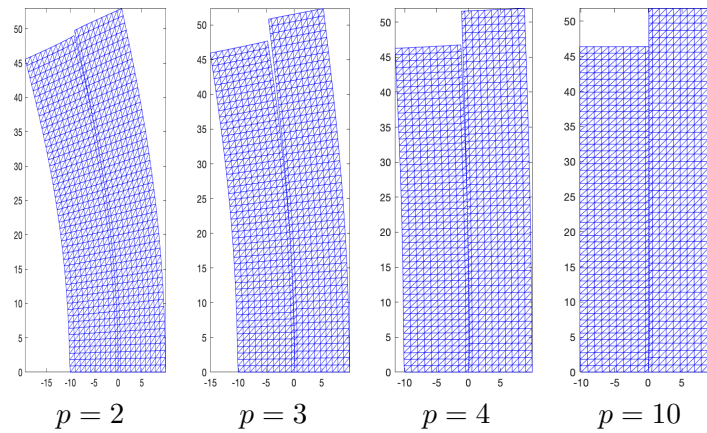


Figure 4: Deformed configurations for various values of p , obtained using the proposed fictitious domain decomposition method

6.3 Scalability

To study the numerical behavior of the proposed fictitious domain decomposition method, the initial mesh of Figure 4 is successively refined to produce meshes with 40×101 , 80×201 , 160×401 and 320×801 nodes. We report in Table 1 the number of iterations and the

CPU time (in Seconds) versus the number of unknowns. We first notice that the number of iterations, for a fixed value of p , is virtually independent of the mesh size. We also notice that the number of iterations is strongly related to the value of p . For $p = 2$, the functional $J + J_\Gamma$ is quadratic and strongly convex, then the conjugate gradient algorithm theoretically converges in a finite number of steps. For $p > 2$, $J + J_\Gamma$ is a general nonlinear functional and the conjugate gradient converges, theoretically, in infinite number of iterations.

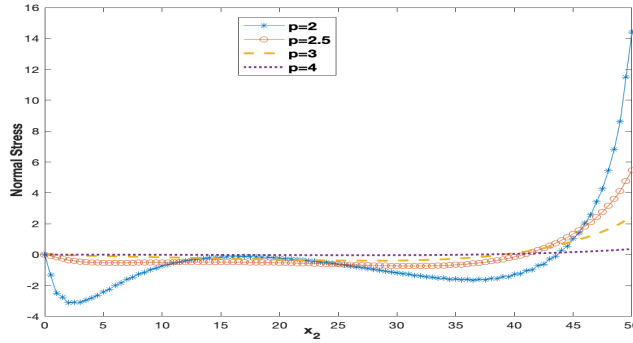


Figure 5: Normal stress distribution on Γ

Mesh nodes $m \times n$	$p = 2$		$p = 3$		$p = 4$		$p = 10$	
	IT	CPU	IT	CPU	IT	CPU	IT	CPU
20×51	8	0.06	61	0.13	299	0.42	21	0.09
40×101	8	0.07	61	0.25	352	1.41	21	0.13
80×201	8	0.28	64	1.51	455	9.99	21	0.61
160×401	8	2.09	59	10.78	379	65.33	21	4.35
320×801	8	13.14	74	84.96	408	450.11	21	27.49

Table 1: Performance of Algorithm 3: number of iterations (IT) and CPU times in Seconds (CPU).

7 Conclusion

We have studied a fictitious domain decomposition method for a nonlinearly bonded structure. Numerical experiments show that the proposed method is numerically scalable, with respect to the mesh size for a fixed value of p . For $p = 2$ or for large values of p , the number of iterations required for convergence is relatively small. For other values of p , the number of iterations required for convergence can become large, since the convergence of the conjugate gradient method in a finite number of iterations is no longer guaranteed for general non linear functions. Further work is underway to improve the proposed Uzawa conjugate gradient method by using preconditioning and restart techniques.

Acknowledgment

The authors are very grateful to the anonymous referees for their helpful and valuable suggestions and remarks, which greatly improved the earlier version of this paper.

References

- [1] AREIAS P.M.A. and BELYTSCHKO T. A comment on the article *a finite element method for the simulation of strong and weak discontinuities in solid mechanics* by A. Hansbo and P. Hansbo [Comput. Methods Appl. Mech. Engrg 193 (2004) 3523-2540]. *Comput. Methods Appl. Mech. Engrg.*, 195:1275–1276, 2006.
- [2] BARBOSA H.J.C and HUGHES T.J.R. The finite element method with Lagrange multipliers on the boundary: circumventing the Babuška—Brezzi condition. *Comput. Methods Appl. Mech. Engrg.*, 85:109–128, 1991.
- [3] BARBOSA H.J.C and HUGHES T.J.R. Boundary Lagrange multipliers in finite element methods: error analysis in natural norms. *Numer. Math.*, 62:1–15, 1992.
- [4] BODART O., CAYOL V., COURT S. and KOKO J. XFEM-based fictitious domain method for linear elasticity model with crack. *SIAM J. Sci. Comput.*, 38:219–246, 2016.
- [5] BRESCH D. A direct asymptotic analysis on a nonlinear model with thin layers. *Ann. Univ. Ferrara - Sez. VII - Sec. Mat.*, 49:359–373, 2003.
- [6] BRESCH D. and KOKO J. An optimization-based domain decomposition method for nonlinear wall laws in coupled systems. *Math. Models Methods Appl. Sci.*, 14(7):1085–1101, 2004.
- [7] BURMAN E. and HANSBO P. Fictitious domain finite element methods using cut elements: I a stabilized Lagrange multiplier method. *Comput. Methods Appl. Mech. Engrg.*, 199:2680–2686, 2010.
- [8] CANUTO C. and URBAN K. Adaptive optimization of convex functionals in Banach spaces. *SIAM J. Numer. Anal.*, 42:2043–2075, 2005.
- [9] EKELAND I. and Temam R. *Convex Analysis and Variational Problems*. SIAM, Philadelphia, USA, 1999.
- [10] FEISTAUER M. and NAJZAR K. Finite element approximation of a problem with a non-linear Newton boundary condition. *Numer. Math.*, 78:403–425, 1998.
- [11] GEYMONAT G., KRASUCKI F., MARINI D. and VIDRASCU M. A domain decomposition method for bonded structures. *Math. Models Methods Appl. Sci.*, 8(8):1387–1402, 1998.

- [12] GLOWINSKI R. and MAROCCO A. Sur l'approximation par éléments finis d'ordre un, et la résolution par pénalisation–dualité, d'une classe de problèmes de Dirichlet non linéaires. *RAIRO Anal. Num.*, 9(2):41–76, 1975.
- [13] GLOWINSKI R., PAN T.-W. and PERIAUX J. Distributed Lagrange multiplier methods for incompressible viscous flow around moving rigid bodies. *Comput. Methods. Appl. Mech. Engrg.*, 151(1-2):181–184, 1998.
- [14] GLOWINSKI R., PAN T.-W., HESLA T.I. and JOSEPH D. A distributed Lagrange multiplier/fictitious domain method for the simulation of flow around moving rigid bodies: application to particulate flow. *Comput. Methods. Appl. Mech. Engrg.*, 184(2-4):241–267, 2000.
- [15] HANSBO A. and HANSBO P. A finite element method for the simulation of strong and weak discontinuities in solid mechanics. *Comput. Methods Appl. Mech. Engrg.*, 193:3523–3540, 2004.
- [16] HASLINGER J. and RENARD Y. A new fictitious domain approach inspired by the extended finite element method. *SIAM J. Numer. Anal.*, 47:1474–1499, 2009.
- [17] KOKO J. An optimization based domain decomposition method for a bonded structure. *Math. Models Methods Appl. Sci.*, 12(6):857–870, 2002.
- [18] KOKO J. Convergence analysis of optimization-based domain decomposition methods for a bonded structure. *Appl. Numer. Math.*, 58:69–87, 2008.
- [19] KOKO J. A MATLAB mesh generator for the two-dimensional finite element method. *Appl. Math. Comput.*, 250:650–664, 2015.
- [20] KOKO J. Fast MATLAB assembly of FEM matrices in 2D and 3D using cell array approach. *Int. J. Model. Simul. Sci. Comput.*, 7, 2016.
- [21] LIONS J.-L. *Quelques Méthodes de Résolution des Problèmes aux Limites Non Linéaires*. Dunod, Paris, 1969.
- [22] MOËS M., DOLBOW J. and BELYTSCHKO T. A finite element method for crack growth without remeshing. *Internat. J. Numer. Methods Engrg.*, 46:131–159, 1999.
- [23] ROCKAFELLAR T. *Convex Analysis*. Princeton University Press, 1970.
- [24] SUQUET P. Discontinuities and plasticity. In MOREAU J.J. and PANAGIOTOPOULOS P.D., editors, *Nonsmooth Mechanics and Applications*, volume 302 of *CISM courses and lectures*, pages 279–340. Springer, 1988.